PROCEEDINGS OF SCIENCE

New gauge-independent transition dividing the confinement phase in the lattice gauge-adjoint scalar model

Akihiro Shibata[a,b,*] **and Kei-Ichi Kondo**[c]

[a] *Computing Research Center, High Energy Accelerator Research Organization (KEK), Tsukuba 305-0801,Japan*

[b] *Department of Accelerator Science, SOKENDAI (The Graduate Univercity for Advanced Studies), Tsukuba 305-0801, Japan*

[c] *Department of Physics, Graduate School of Science, Chiba University, Chiba 263-8522, Japan*

E-mail: akihiro.shibata@kek.jp, kondok@faculty.chiba-u.jp

The lattice gauge-scalar model with the scalar field in the adjoint representation of the gauge group has two completely separated confinement and Higgs phases according to the preceding studies based on numerical simulations which have been performed in the specific gauge fixing based on the conventional understanding of the Brout-Englert-Higgs mechanism.

In this talk, we reexamine this phase structure in the gauge-independent way based on the numerical simulations for the model with SU(2) gauge group performed without any gauge fixing which is motivated to confirm the recently proposed gauge-independent Brout-Englert-Higgs mechanics for the mass of the gauge field without relying on any spontaneous symmetry breaking. For this purpose we investigate correlation functions between gauge-invariant operators obtained by combining the original adjoint scalar field and the new field called the color-direction field constructed from the gauge field based on the gauge-covariant gauge-field decomposition due to Cho-Duan-Ge-Shabanov and Faddeev-Niemi. We reproduce gauge-independently the transition line separating confinement and Higgs phase, and discover surprisingly a new transition line that divides the confinement phase into two parts. Finally, we discuss the physical meaning of the new transition and implications to confinement mechanism. This talk is based on the preprint [1]

The 40th International Symposium on Lattice Field Theory (Lattice 2023)
July 31st - August 4th, 2023
Fermi National Accelerator Laboratory

*Speaker

PoS(LATTICE2023)373

1. Introduction

We investigate the gauge-scalar model to clarify the mechanism of confinement in the Yang-Mills theory in the presence of matter fields and also non-perturbative characterization of the Brout-Englert-Higgs (BEH) mechanism [2] providing the gauge field with the mass, in the gauge-independent way.

For concreteness, we reexamine the lattice $SU(2)$ gauge-scalar model with a radially-fixed scalar field (no Higgs mode) which transforms according to the adjoint representation of the gauge group $SU(2)$ without any gauge fixing. In fact, this model was investigated long ago in [3] by taking a specific gauge, say unitary gauge, based on the traditional characterization for the BEH mechanism to identify the Higgs phase. It is a good place to recall the traditional characterization of the BEH mechanism: If the original continuous gauge group is spontaneously broken, the resulting massless Nambu-Goldstone particles are absorbed into the gauge field to provide the gauge field with the mass. In the perturbative treatment, such a spontaneous symmetry breaking is signaled by the non-vanishing vacuum expectation value of the scalar field. However, this is impossible to realize on the lattice unless the gauge fixing condition is imposed, since gauge non-invariant operators have vanishing vacuum expectation value on the lattice without gauge fixing due to the Elitzur theorem [4]. This traditional characterization of the BEH mechanism prevents us from investigating the Higgs phase in the gauge-independent way.

This difficulty can be avoided by using the *gauge-independent description of the BEH mechanism* proposed recently by one of the authors [5, 6], which *needs neither the spontaneous breaking of gauge symmetry*, nor the *non-vanishing vacuum expectation value of the scalar field*. Then we can give a *gauge-independent definition of the mass for the gauge field* resulting from the BEH mechanism. Therefore, we can study the Higgs phase in the gauge-independent way on the lattice without gauge fixing based on the lattice construction of gauge-independent description of the BEH mechanism. Consequently, we can perform numerical simulations without any gauge-fixing and compare our results with those of the preceding result [3] obtained in a specific gauge. Indeed, our gauge-independent study reproduces the transition line separating Higgs and confinement phases obtained by [3] in a specific gauge.

2. Lattice $SU(2)$ gauge-scalar model with a scalar field in the adjoint representation

The $SU(2)$ gauge-scalar model with a radially-fixed scalar field in the adjoint representation is given on the lattice with a lattice spacing ϵ by the following action with two parameters β and γ:

$$S_{\rm GS} := \frac{\beta}{2}\sum_x \sum_{\mu<\nu} \mathrm{tr}\left\{\left(\mathbf{1}-U_{x,\mu}\right)\left(\mathbf{1}-U^\dagger_{x,\mu}\right)\right\} + \frac{\gamma}{2}\sum_{x,\mu}\mathrm{tr}\left((D^\epsilon_\mu[U]\boldsymbol{\phi}_x)^\dagger (D^\epsilon_\mu[U]\boldsymbol{\phi}_x)\right)\,, \tag{1}$$

where $U_{x,\mu\nu} := U_{x,\mu}U_{x+\epsilon\hat{\mu},\nu}U^\dagger_{x+\epsilon\hat{\nu},\mu}U^\dagger_{x,\nu}$ represents plaquettes with a gauge variable $U_{x,\mu} := \exp(-ig\epsilon\mathscr{A}_{x,\mu}) \in SU(2)$ on a link $\langle x,\mu\rangle$, $\boldsymbol{\phi}_x = \phi^A_x\sigma^A \in su(2)-u(1)$ $(A=1,2,3)$ represents a scalar field on a site x in the adjoint representation subject to the radially-fixed condition: $\boldsymbol{\phi}_x\cdot\boldsymbol{\phi}_x = \phi^A_x\phi^A_x = 1$, and $D^\epsilon_\mu[U]\boldsymbol{\phi}_x$ represents the covariant derivative in the adjoint representation defined with ϵ being the lattice spacing as

$$D^\epsilon_\mu[U]\boldsymbol{\phi}_x := U_{x,\mu}\boldsymbol{\phi}_{x+\epsilon\hat{\mu}} - \boldsymbol{\phi}_x U_{x,\mu}\,. \tag{2}$$

This action reproduces in the naive continuum limit $\epsilon\to 0$ the continuum gauge-scalar theory with a radially-fixed scalar field $|\phi(x)| = v$ and a gauge coupling constant g where $\beta = 4/g^2$ and $\gamma = v^2/2$. Note that this action is invariant under the gauge transformation $\Omega_x \in SU(2)$ as

$$U_{x,\mu}\to\Omega_x U_{x,\mu}\Omega^\dagger_{x+\epsilon\hat{\mu}} = U'_{x,\mu},\quad \boldsymbol{\phi}_x\to\Omega_x\boldsymbol{\phi}_x\Omega^\dagger_x = \boldsymbol{\phi}'_x \tag{3}$$

In what follows we take the lattice spacing $\epsilon = 1$ in the numerical simulation.

The numerical simulation can be performed by updating link variables and scalar fields alternately. For link variable $U_{x,\mu}$ we can apply the standard HMC algorithm. While for scalar field we reparametrized the variable $\boldsymbol{\phi}_x$ according to the adjoint-orbit representation:

$$\boldsymbol{\phi}_x := Y_x \sigma^3 Y_x^\dagger, \quad Y_x \in SU(2), \tag{4}$$

which satisfies the normalization condition $\boldsymbol{\phi}_x \cdot \boldsymbol{\phi}_x = 1$ automatically. Therefore, the Haar measure is replaced by $\prod_x d\boldsymbol{\phi}_x \delta(\boldsymbol{\phi}_x \cdot \boldsymbol{\phi}_x - 1)$ to $\prod_x dY_x$, and we can apply the standard HMC algorithm for the variable Y_x to update configurations of the scalar fields $\boldsymbol{\phi}_x$.

3. gauge-independent analyses of the phase structure

To search for the phase boundary, we measure the expectation value $\langle O \rangle$ of a chosen operator O by changing γ (or β) along the β =const. (or γ =const.) lines. The location of the phase boundary is determined based on two ways: (i) The location at which $\langle O \rangle$ changes from $\langle O \rangle \simeq 0$ to $\langle O \rangle > 0$, (ii) the location at which $\langle O \rangle$ changes abruptly, i.e., the bent, step and gap in the plots of the measurements.

3.1 Action densities for the plaquette and scalar parts

First of all, in order to determine the phase boundary of the model, we measure the Wilson action per plaquette (plaquette-action density) and that of the scalar action per link (scalar-action density):

$$P = \frac{1}{6N_{\rm site}} \sum_x \sum_{\mu<\nu} \frac{1}{2} \mathrm{tr}(U_{x,\mu\nu}) \,, \tag{5}$$

$$M = \frac{1}{4N_{\rm site}} \sum_x \sum_{\mu} \frac{1}{2} \mathrm{tr} \left(\left(D_\mu[U_{x,\mu}] \boldsymbol{\phi}_x \right)^\dagger \left(D_\mu[U_{x,\mu}] \boldsymbol{\phi}_x \right) \right) \,, \tag{6}$$

which are the gauge-invariant version that Brower et al. have adopted in [3] .

3.2 Correlations between the scalar field and the color-direction field through the gauge covariant decomposition

To investigate gauge-independently the phase structure of the gauge-scalar model, we introduce the lattice version [7, 8] of change of variables based on the idea of the *gauge-covariant decomposition of the gauge field*, so called the CDGSFN decomposition [9–12]. For a review, see [13].

In the decomposition, we introduce the site variable $\boldsymbol{n}_x := n_x^A \sigma_A \in su(2) - u(1)$ which is called the color-direction (vector) field, in addition to the original link variable $U_{x,\mu} \in SU(2)$. A link variable $U_{x,\mu}$ is decomposed into two parts: $U_{x,\mu} := X_{x,\mu} V_{x,\mu}$. We identify the lattice variable $V_{x,\mu}$ with a link variable which transforms in the same way as the original link variable $U_{x,\mu}$, and we define the lattice variable $X_{x,\mu}$ such that it transforms in just the same way as the site variable $\boldsymbol{n}_x$:

$$V_{x,\mu} \to \Omega_x V_{x,\mu} \Omega_{x+\mu}^\dagger = V'_{x,\mu} \,, \quad X_{x,\mu} \to \Omega_x X_{x,\mu} \Omega_x^\dagger = X'_{x,\mu} \,, \quad \boldsymbol{n}_x \to \Omega_x \boldsymbol{n}_x \Omega_x^\dagger = \boldsymbol{n}'_x. \tag{7}$$

Such decomposition is obtained by solving the definning equation:

$$D_\mu[V] \boldsymbol{n}_x := V_{x,\mu} \boldsymbol{n}_{x+\mu} - \boldsymbol{n}_x V_{x,\mu} = 0 \,, \quad \mathrm{tr}(\boldsymbol{n}_x X_{x,\mu}) = 0 \,. \tag{8}$$

This defining equation has been solved exactly [7] and the decomposition is obtained uniquly for a given set of link variables $U_{x,\mu}$ once a set of site variables $\boldsymbol{n}_x$ is given. The configurations of the color-direction field $\{\boldsymbol{n}_x^*\}$ are obtained by minimizing the functional:

$$F_{\rm red}[\{\boldsymbol{n}_x\}|\{U_{x,\mu}\}] := \sum_{x,\mu} {\rm tr}\left\{ \left(D_{x,\mu}[U]\boldsymbol{n}_x\right)^\dagger \left(D_{x,\mu}[U]\boldsymbol{n}_x\right)\right\} \tag{9}$$

which we call the *reduction condition*.

Therefore, as a new gauge-invariant order parameter, we propose the scalar-color correlation detected by the scalar-color composite operator:

$$Q = \frac{1}{N_{\rm site}} \sum_x \frac{1}{2}{\rm tr}(\boldsymbol{n}_x^* \boldsymbol{\phi}_x) \ , \quad \{\boldsymbol{n}_x^*\} = \underset{\{\boldsymbol{n}_x\}}{\rm argmin} F_{\rm red}[\{\boldsymbol{n}_x\}|\{U_{x,\mu}\}] \ , \tag{10}$$

where $\{\boldsymbol{n}_x^*\}$ is the color-direction field configuration determined by the reduction condition (9). This has two kinds of ambiguity. One comes from the so-called lattice Gribov copies that are the local minimal solutions of the reduction condition. In order to avoid the local minimal solutions and to obtain the absolute minimum, the reduction condition is solved by using the over-relaxation algorithm and changing the initial values to search for the absolute minimum of the functional. The other comes from the choice of a global sign factor, which originates from the fact: whenever a configuration $\{\boldsymbol{n}_x^*\}$ is a solution, the flipped one $\{-\boldsymbol{n}_x^*\}$ is also a solution, since the reduction functional is quadratic in the color field. To avoid these issues, we propose to use $\langle|Q|\rangle$ and $\langle Q^2\rangle$, which are examined as the order parameters that determine the phase boundary.

4. Lattice result

We perform Monte Carlo simulations on the 16^4 lattice with periodic boundary condition in the gauge-independent way (without gauge fixing). In each Monte Carlo step (sweep), we update link variables $\{U_{x,\mu}\}$ and scalar fields $\{\boldsymbol{\phi}_x\}$ alternately by using the HMC algorithm with integral interval $\Delta\tau = 1$ as explained in the previous section. We take thermalization for 5000 sweeps and store 800 configurations for measurements every 25 sweeps.

First, we try to determine the phase boundary from the plaquette-action density in eq(5) and the scalar-action density in eq(6). Figure 1 shows the results of measurements of the plaquette-action density

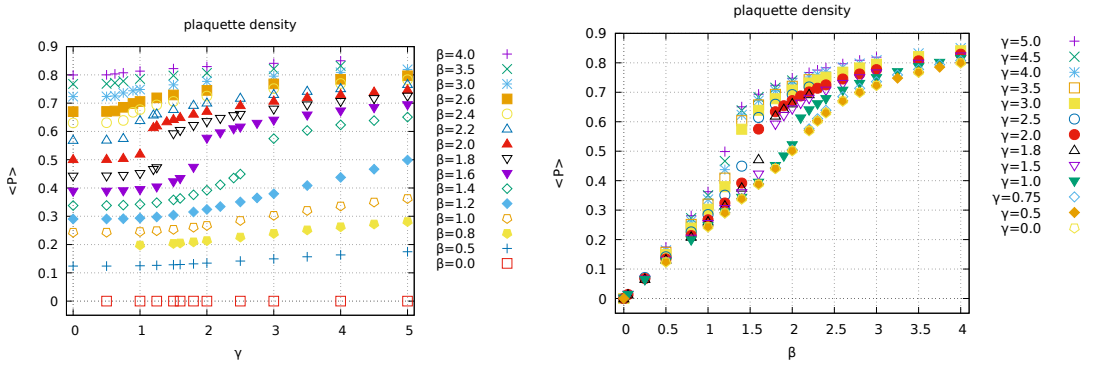

Figure 1: Average of the plaquette-action density $\langle P\rangle$: (Left) $\langle P\rangle$ versus γ on various β = const. lines, (Right) $\langle P\rangle$ versus β on various γ =const. lines.

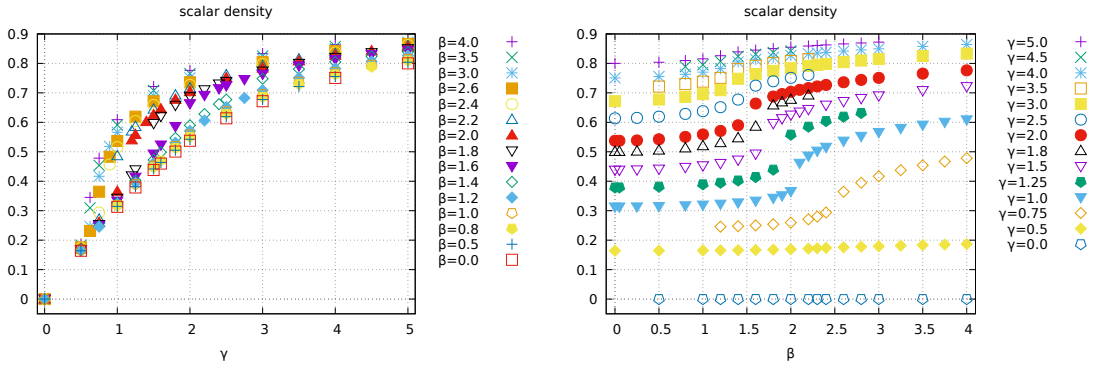

Figure 2: Average of the scalar-action density $\langle M \rangle$: (Left) $\langle M \rangle$ versus γ on various β = const. lines, (Right) $\langle M \rangle$ versus β on various γ =const. lines.

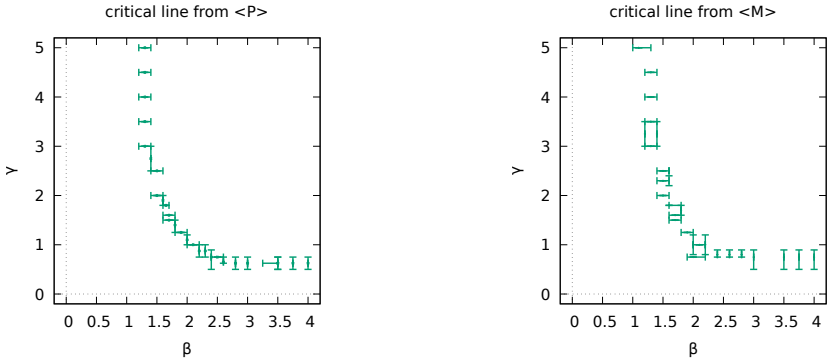

Figure 3: The phase boundary determined by the action densities: (Left) $\langle P \rangle$, (Right) $\langle M \rangle$.

$\langle P \rangle$ in the β–γ plane. The left panel shows the plots of $\langle P \rangle$ along β =const. lines as functions of γ, where error bars are not shown because they are smaller than the size of the plot points. On the other hand, the right panel shows the plots of $\langle P \rangle$ along γ =const. lines as functions of β. Figure 2 shows the results of measurement of the scalar-action density $\langle M \rangle$ in the β–γ plane. The left panel of Fig.2 shows the plots of $\langle M \rangle$ along β =const. lines as functions of γ, while the right panel of Fig.2 shows the plots of $\langle M \rangle$ along γ =const. lines as functions of β.

In Figure 3, we plot the phase boundary determined from the above mesurements. The left panel of Fig.3 shows the phase boundary determined from $\langle P \rangle$, and the right panel of Fig.3 shows the phase boundary determined from the scalar-action density $\langle M \rangle$. The location of the phase boundary is determined by a gap or step in the plots of measurements. The interval between the two simulation points in each plot corresponds to the short line with ends. The error bars in the phase boundary are due to the spacing of the simulation points. It should be noticed that the two phase boundaries determined from $\langle P \rangle$ and $\langle M \rangle$ are consistent within accuracy of numerical calculations. Thus we find that the gauge-independent numerical simulations reproduce the critical line obtained by Brower et al. [3].

Next, we try to determine the phase bundery from the scalar-color correlation in eq.(10). Figure 4 shows the measurements of $\langle |Q| \rangle$. The left panel shows plots of $\langle |Q| \rangle$ versus γ along various β =const. lines, while the right panel shows plots of $\langle |Q| \rangle$ versus β along various γ =const. lines. Figure 5, on the other hand, shows the measurements of $\langle Q^2 \rangle$ in the same manner as $\langle |Q| \rangle$. The left panel shows plots of $\langle Q^2 \rangle$ versus γ along various β =const. lines, while the right panel shows plots of $\langle Q^2 \rangle$ versus β along

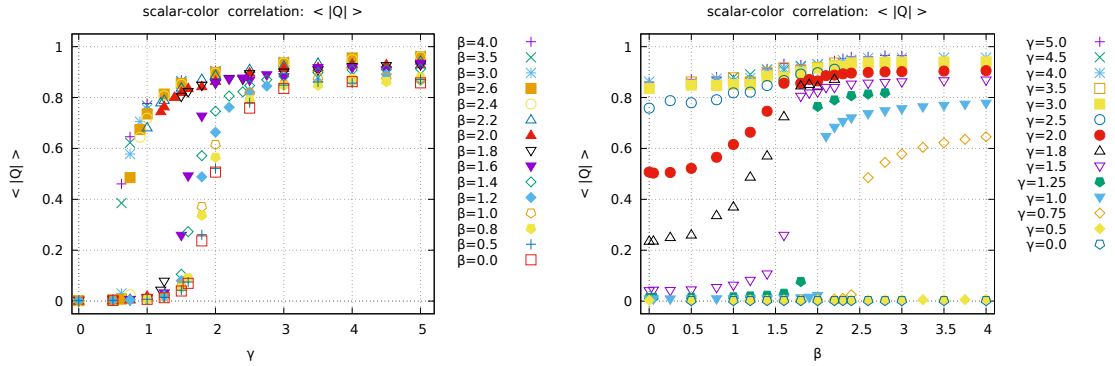

Figure 4: Average of the scalar-color composite field $\langle|Q|\rangle$: (Left) $\langle|Q|\rangle$ versus γ on various β =const. lines, (Right) $\langle|Q|\rangle$ versus β on various γ =const. lines.

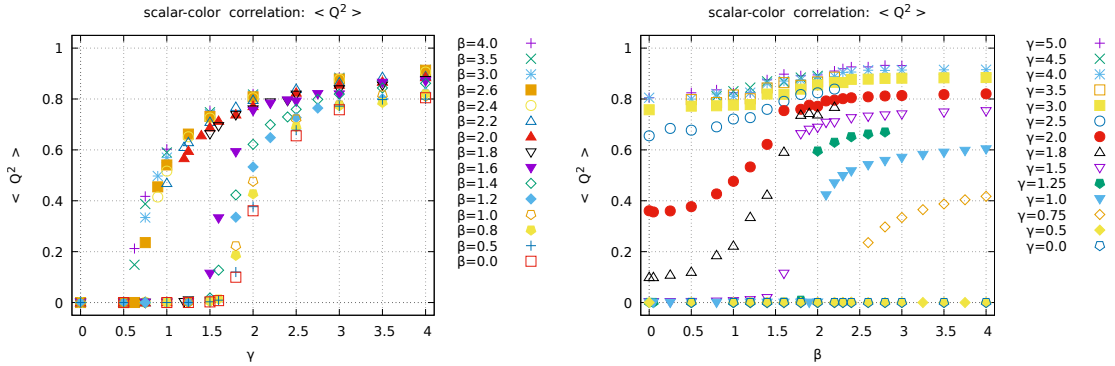

Figure 5: Average of the squared scalar-color composite field $\langle Q^2\rangle$: (Left) $\langle Q^2\rangle$ versus γ on various β =const. lines, (Right) $\langle Q^2\rangle$ versus β on various γ =const. lines.

various γ =const. lines.

Figure 6 shows the phase boundary (critical line) determined by $\langle|Q|\rangle$ and $\langle Q^2\rangle$. The left panel of Fig.6 shows the phase boundary determined from $\langle|Q|\rangle$. The right panel of Fig.6 shows the phase boundary determined from $\langle Q^2\rangle$. The purple boundary indicates that $\langle|Q|\rangle$ changes from $\langle|Q|\rangle \simeq 0$ to $\langle|Q|\rangle > 0$ (or $\langle Q^2\rangle$ changes from $\langle Q^2\rangle \simeq 0$ to $\langle Q^2\rangle > 0$). The black boundary corresponds to the location at which $\langle|Q|\rangle$ (or $\langle Q^2\rangle$) has gaps. The orange boundary corresponds to the location at which $\langle|Q|\rangle$ (or $\langle Q^2\rangle$) bends. The results in Fig.6 are consistent with each other.

Fig.6 shows not only the phase boundary that divides the phase diagram into two phases, so-called the Higgs phase and the confinement phase, but also the new boundary that divides the confinement phase into two different parts. It should be remarked that this finding owes much to gauge-independent numerical simulations and their analyses, and this new results can only be established through our framework.

5. Understanding the new phase structure

Finally, we discuss why the above phase structure should be obtained and how the respective phase is characterized from the physical point of view. Figure 7 shows the schematic view of the resulting phase structure. In the region below the new critical line $\gamma < \gamma_c(\beta)$ where the average $\langle|Q|\rangle$ takes very small or vanishing values, the color direction field $\boldsymbol{n}_x$ takes various possible directions with no specific direction in color space, which we call the disordered phase. The effect of the scalar field would be relatively small

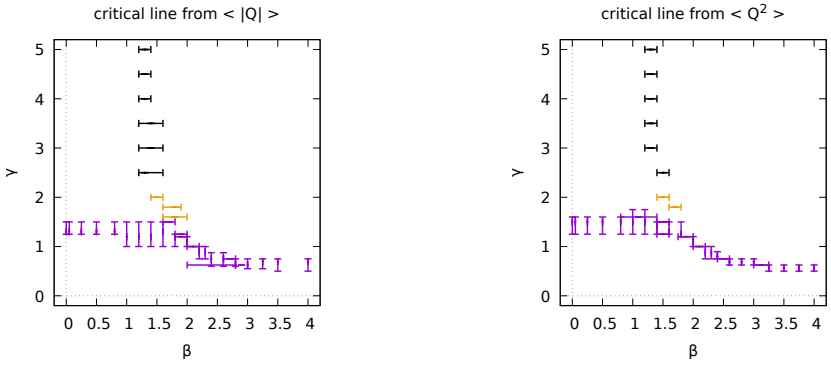

Figure 6: Phase boundary determined from color-scalar correlation: (Left) $\langle|Q|\rangle$, (Right) $\langle Q^2\rangle$.

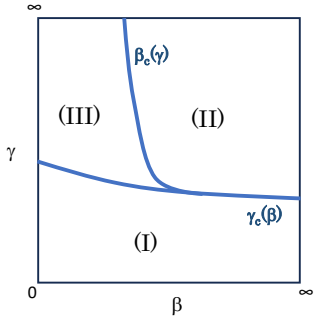

Figure 7: Phase structure of the lattice SU(2) gauge-adjoint scalar model: (I) Confinement phase, (II) Higgs phase, (III) Confinement phase.

and confinement would occur in the way similar to the pure $SU(2)$ gauge theory ($\gamma = 0$), which we call Confinement phase (I). In the region above the critical line, including the two phases: Higgs phase (II) $\gamma > \gamma_c(\beta)$, $\beta > \beta_c(\gamma)$ and Confinement phase (III) $\gamma > \gamma_c(\beta)$, $\beta < \beta_c(\gamma)$, the average $\langle|Q|\rangle$ takes the non-vanishing value, the color-direction field $\boldsymbol{n}_x$ correlates strongly with the given scalar field $\boldsymbol{\phi}_x$ which tends to align to an arbitrary but a specific direction as expected from the spontaneous symmetry breaking, which we call the orderd phase.

In the Confinement phase (I), confinement is expected to occur due to vacuum condensations of non-Abelian magnetic monopoles [14]. Here the non-Abelian magnetic monopole should be carefully defined gauge-independently using the gauge-independent method, which is actually realized by extending the gauge-covariant decomposition of the gauge field, see [13] for a review.

In the Higgs phase (II), the off-diagonal gauge fields for the modes $SU(2)/U(1)$ become massive due to the BEH mechanism, which is a consequence of the (partial) spontaneous symmetry breaking $SU(2) \to U(1)$ according to the conventional understanding of the BEH mechanism, although this phenomenon is also understood gauge-independently based on the new understanding of the BEH mechanism without the spontaneous symmetry breaking [5]. Therefore, the diagonal gauge field for the mode $U(1)$ always remains massless everywhere.

In the other Confinement phase (III), the gauge fields become massive due to different physical origins. Indeed, the gauge fields become massive due to self-interactions among the gauge fields, as in the phase (I). In the phase (III), no massless gauge field exists and the gauge fields for all the modes become

massive, which is consistent with the belief that the original gauge symmetry $SU(2)$ would be kept intact and not spontaneously broken.

In the Confinement phases (I) and (III) there occur magnetic monopole condensations which play the dominant role in explaining quark confinement based on the dual superconductor picture [14–18] while in the Higgs phase (II) there are no magnetic monopole condensations and confinement would not occur. However, it should be remarked that the origin of magnetic monopoles is different in the two regions, (I) and (III). In phase (III) the magnetic monopole is mainly originated from the adjoint scalar field just like the 't Hooft-Polyakov magnetic monopole in the Georgi-Glashow model [19]. In phase (I) the magnetic monopole is constructed from the gauge field. Indeed, the magnetic monopole can be constructed only from the gauge degrees of freedom, which is explicitly constructed from the color direction field in the gauge-independent way [13].

6. Summary and discussion

We have investigated the lattice $SU(2)$ gauge-scalar model with the scalar field in the adjoint representation of the gauge group in a gauge-independent way. We have reexamined this phase structure in the gauge-independent way based on the numerical simulations performed without any gauge fixing, which should be compared with the preceding studies [3]. This is motivated to confirm the recently proposed gauge-independent BEH mechanics for giving the mass of the gauge field without relying on any spontaneous symmetry breaking [5, 6]. For this purpose we have investigated correlation functions between gauge-invariant operators obtained by combining the original adjoint scalar field and the new field called the color-direction field which is constructed from the gauge field based on the gauge-covariant decomposition of the gauge field due to CDGSFN.

We have reproduced gauge-independently the transition line separating the confinement phase and the Higgs phase which was obtained in [3]. We have shown surprisingly the existence of a new transition line that divides completely the confinement phase into two parts. We have discussed the physical meaning of the new transition and implications to confinement mechanism. More discussions on the physical properties of the respective phase will be given in subsequent papers. In particular, it is quite important to study whether or not the new phase (III) is a lattice artefact and survives the continuum limit.

The result obtained in this paper should be compared with the lattice $SU(2)$ gauge-scalar model with the scalar field in the fundamental representation of the gauge group in a gauge-independent way. This model has a single confinement-Higgs phase where two confinement and Higgs regions are analytically continued according to the preceding studies [20, 21]. Even in this case, it is shown [22] that the composite operator constructed from the original fundamental scalar field and the color-direction field can discriminate two regions which indicates the existence of the transition line seperating the confinement-Higg phase into completely different two phases, Confinement phase and Higgs phase.

Acknowledgement

This work was supported by Grant-in-Aid for Scientific Research, JSPS KAKENHI Grant Number (C) No.23K03406. The numerical simulation is supported by the Particle, Nuclear and Astro Physics Simulation Program No.2022-005 (FY2022) of Institute of Particle and Nuclear Studies, High Energy Accelerator Research Organization (KEK). This research was supported in part by the Multidisciplinary Cooperative Research Program in CCS, University of Tsukuba.

References

[1] A. Shibata and K-I .Kondo , arXiv:2307.15953 [hep-lat]; KEK Preprint 2023-24, CHIBA-EP-258

[2] P.W. Higgs, Phys. Lett.**12**, 132 (1964). Phys. Rev. Lett. **13**, 508 (1964).
F. Englert and R. Brout, Phys. Rev. Lett.**13**, 321 (1964).

[3] R.C. Brower, D.A. Kessler, T. Schalk, H. Levine, M. Nauenberg, Phys. Rev. D**25**, 3319 (1982).

[4] S. Elitzur, Phys. Rev. D**12**, 3978 (1975).

[5] K.-I. Kondo, Phys. Lett. B **762**, 219 (2016). arXiv:1606.06194 [hep-th]

[6] K.-I. Kondo, Eur. Phys. J. C **78**, 577 (2018). arXiv:1804.03279 [hep-th]

[7] A. Shibata, K.-I.Kondo, T.Shinohara, Phys. Lett.B**691**, 91 (2010). arXiv:0706.2529 [hep-lat]

[8] A. Shibata, S. Kato, K.-I. Kondo, T. Murakami, T. Shinohara, S. Ito, Phys. Lett. B**653**, 101 (2007). arXiv:0706.2529 [hep-lat]

[9] Y.M. Cho, Phys. Rev. D**21**, 1080 (1980). Phys. Rev. D**23**, 2415 (1981).

[10] Y.S. Duan and M.L. Ge, Sinica Sci. **11**, 1072 (1979).

[11] S.V. Shabanov, Phys. Lett. B**463**, 263 (1999). [hep-th/9907182]

[12] L.D. Faddeev and A.J. Niemi, Phys. Rev. Lett. **82**, 1624 (1999). [hep-th/9807069];
L.D. Faddeev and A.J. Niemi, Nucl. Phys. B**776**, 38 (2007). [hep-th/0608111]

[13] K.-I. Kondo, S. Kato, A. Shibata and T. Shinohara, Phys. Rept. **579**, 1–226 (2015). arXiv:1409.1599 [hep-th]

[14] Y. Nambu, Phys. Rev. D**10**, 4262 (1974).
G. 't Hooft, in: High Energy Physics, edited by A. Zichichi (Editorice Compositori, Bologna, 1975).
S. Mandelstam, Phys. Rept. **23**, 245 (1976).

[15] G. 't Hooft, Topology of the gauge condition and new confinement phases in non-Abelian gauge theories, Nucl. Phys. B**190** [FS3], 455 (1981).

[16] Z.F. Ezawa and A. Iwazaki, Phys. Rev. D**25**, 2681 (1982).

[17] T. Suzuki and I. Yotsuyanagi, Phys. Rev. D**42**, 4257 (1990).

[18] K. Amemiya and H. Suganuma, Phys. Rev. D**60**, 114509 (1999). [hep-lat/9811035]

[19] A.M. Polyakov, Nucl. Phys. B**120**, 429 (1977).

[20] K. Ostewalder and E. Seiler, Annls. Phys **110**, 440 (1978).

[21] E. Fradkin and S.H. Shenker, Phys. Rev. D**19**, 3682 (1979).

[22] R. Ikeda, S. Kato, K.-I. Kondo, A. Shibata, arXiv:2308.13430 [hep-lat], CHIBA-EP-259, KEK Preprint 2023-27